metals

MDPI

Article

Effect of Post-Deposition Thermal Treatments on Tensile Properties of Cold Sprayed Ti6Al4V

Dibakor Boruah [1,2,*], Xiang Zhang [2], Philip McNutt [1], Raja Khan [3] and Henry Begg [1]

[1] Surface, Corrosion and Interface Engineering, TWI Ltd., Cambridge CB21 6AL, UK
[2] Centre for Manufacturing and Materials Engineering, Faculty of Engineering, Environment and Computing, Coventry University, Coventry CV1 5FB, UK
[3] Thermal Processing Technologies, TWI Ltd., Cambridge CB21 6AL, UK
* Correspondence: d.boruah@twi.co.uk

Abstract: This study aims at investigating the effect of various post-deposition thermal treatments on improving tensile properties of cold spray (CS) deposited titanium alloy Ti6Al4V. Dogbone-shaped tensile specimens were designed considering two application scenarios: 'fully CS' specimens, and 'CS repair' specimens. For both specimen types, tests were carried out in four conditions: (i) as-deposited (AD), and after three different thermal treatments, i.e., (ii) solution treatment and ageing (STA), (iii) hot isostatic pressing (HIP), and (iv) HIP followed by STA (HIP + STA). Complementary to tensile testing, characterisation of CS deposited material was also carried out in terms of microstructure and hardness. The STA process resulted in the highest improvement in ultimate tensile strength by more than 200%, reaching 868 MPa for 'fully CS' and 951 MPa for 'CS repair' specimens. However, no appreciable improvement in elongation at failure was achieved, highest being 1.2% for 'fully CS' after STA, and 4.3% for 'CS repair' after HIP. In addition to experimental investigation, a comprehensive collection of data from the open literature on the effect of various thermal treatments on improving the tensile properties of CS Ti6Al4V deposits is reported and discussed.

Keywords: additive manufacturing; cold spray; repair; Ti6Al4V; thermal treatments; tensile properties

Citation: Boruah, D.; Zhang, X.; McNutt, P.; Khan, R.; Begg, H. Effect of Post-Deposition Thermal Treatments on Tensile Properties of Cold Sprayed Ti6Al4V. *Metals* **2022**, *12*, 1908. https://doi.org/10.3390/met12111908

Academic Editor: Alessio Silvello

Received: 8 October 2022
Accepted: 31 October 2022
Published: 7 November 2022

1. Introduction

Titanium alloy Ti6Al4V is a commonly used material among the various titanium alloys, with growing demand due to its well-known properties such as high specific strength and stiffness, excellent fatigue and corrosion resistance, good thermal stability, biocompatibility, etc. Moreover, mechanical properties for this α + β titanium alloy can be tailored to the intended applications by controlling the microstructure through different thermal treatments. Ti6Al4V has applications in a wide range of sectors including the aerospace, automotive, marine, power generation, sports, and biomedical industries. Ti6Al4V is extensively used in aircraft components such as engine parts, hydraulic tubing, landing gear, load-bearing airframe structures, etc. [1–3].

Aircraft components are susceptible to various in-service damage, such as foreign and domestic object damage (FOD and DOD), fretting/galling wear, fatigue cracks, etc. In most cases, repair or remanufacturing is a more sustainable solution than replacement, which has become more promising with the advancement of the solid-state Cold Spray (CS) additive deposition technique. In CS, powder particles are propelled to reach a critical velocity by a supersonic jet of preheated, compressed gas such as nitrogen (N_2), helium (He), or a mixture of N_2 + He at a temperature lower than the melting point of the deposited material. The high-velocity impact of the powder particles and their associated severe plastic deformation result in deposited layers on a substrate. Due to lower operating temperature in the CS process, the detrimental effects associated with high-temperature processes (oxidation, melting and solidification, phase transformations, compositional changes, heat-affected zones, high tensile residual stresses, etc.) can be minimized or even

eliminated. The CS process is therefore potentially suitable for repairing high-temperature oxidation sensitive materials such as titanium alloys. In addition to repair applications, the CS process is an emerging solid-state freeform fabrication technology that has recently been adopted for AM applications, commonly known as cold spray additive manufacturing (CSAM) [4,5]. With the recent technological advancements, the CS process offers a unique opportunity for the near-net-shape manufacturing of complex titanium structures with minimal waste [6,7]. However, repairing or manufacturing aerospace-grade materials is challenging, as sufficient structural integrity is a mandatory requirement for load-bearing structural components.

Cold spraying of Ti6Al4V has been widely studied by many researchers in the past two decades, especially in terms of understanding the effect of process conditions on the characteristics of CS deposits. However, there is limited research on the mechanical properties of CS Ti6Al4V under static and fatigue loading conditions.

Tensile properties of CS Ti6Al4V were reported by many researchers, however, most of them were performed by either the Micro Flat Tensile (MFT) [3,8–11] or Tubular Coating Tensile (TCT) test [9]. The former increases the sensitivity of the test results due to its smaller dimensions unless a special effort is made to ensure the reliability of the test results [7]. Therefore, resulting stress–strain curves are not always a true representation of its engineering strain, as there were many instances where strain values at failure were overestimated [3,10]. The TCT test cannot generate a stress–strain curve to acquire properties such as elongation and elastic modulus [12]. Tensile properties measured by the ASTM E8 standard were reported in [13–16] for fully CS deposited Ti6Al4V material, however, there is no published work on tensile properties of CS repairs.

In the as-deposited (AD) condition, CS Ti6Al4V possesses considerable process-induced defects/porosity, microstructural inhomogeneity, residual stresses, etc., which can adversely affect the structural integrity of parts manufactured or repaired by CS Ti6Al4V. Therefore, it is necessary to perform some thermal treatments that homogenise the microstructure, reduce porosity, relieve residual stresses, and ultimately improve the mechanical properties. The effect of thermal treatments on the characteristics of CS Ti6Al4V deposits was investigated in many studies; most of them used various annealing treatments [3,8,13,17–21]. However, there is limited research reporting the effect of solution treatment and ageing (STA) [22] and hot isostatic pressing (HIP) [13–16] on the mechanical properties of CS Ti6Al4V.

This study was aimed to investigate the tensile properties of CS deposited Ti6Al4V alloy for repairs and additive manufacturing (AM) applications. An attempt has been made to improve the microstructure and enhance mechanical properties of CS Ti6Al4V deposits via three different thermal treatments: (i) STA, (ii) HIP, and (iii) HIP + STA. Subsequently, they have been characterised in terms microstructure, hardness, tensile properties, and fractography.

2. Materials and Methods

2.1. Substrate Material and Feedstock Powder

A commercially available gas atomised Ti6Al4V powder was used (grade 5; size: d_{10} 17 µm, d_{50} 23 µm, d_{90} 32 µm; apparent density 2.44 g/cm^3 and tapped density 2.82 g/cm^3), received from LPW Technology Ltd., Cheshire, UK. The substrate material used in this study was a mill annealed Ti6Al4V (grade 5), supplied by Dynamic Metals Ltd., Bedfordshire, UK. More information on the materials used can be found in [23–25].

2.2. Cold Spray System and Process Conditions

All specimens were manufactured using Impact Innovation 5/11 High-Pressure CS System at TWI Ltd., Cambridge, UK. Key process parameters used for CS are shown in Table 1.

Table 1. Spraying conditions used to deposit Ti6Al4V [7].

CS system setup	Gun	CS system	Impact 5/11
		Nozzle	T24-SiC
		Pre-chamber	Long (128.6 mm)
		Process gas	Nitrogen (N_2)
		Gas pressure (MPa)	5
		Gas temperature (°C)	1100
	Powder feeder	Dosing disk rotation speed (rpm)	3
		Powder feed rate (g/min)	24.67
		Carrier gas flow rate (m^3/h)	3
		Nozzle cooling medium	Water
Robot and toolpath setup		Gun traverse or scanning speed (mm/s)	500
		Track spacing (mm)	2
		Spray angle (°)	90
		Standoff distance (mm)	30
		Toolpath pattern	Cross-hatch

2.3. Post-Deposition Thermal Treatments

Employing optimum process conditions can significantly reduce process-induced porosity in CS Ti6Al4V deposits. However, such reductions are not necessarily sufficient to achieve adequate mechanical properties. Therefore, thermal treatment is an attractive option to reduce or even eliminate pores, homogenise microstructure, relieve residual stresses, increase inter-particle metallurgical bonding, and thereby enhance mechanical properties of CS deposited material [11,13,14,17]. Thus, three different thermal treatments were chosen to explore in this study:

(i) Solution treatment and ageing (STA): STA is an established technique that can improve the strength of Ti6Al4V alloy while maintaining its ductility. A wide range of microstructure and mechanical properties can be achieved in α-β alloys after STA treatment, which originates in the instability of high-temperature β phase at lower temperatures. Heating α-β alloy to the solution-treating temperature (generally 25–85 °C below β-transus) increases the ratio of β to α phase. This partitioning of phases is maintained following quenching. Subsequent ageing treatment (425–650 °C) promotes the decomposition of unstable β phase and any martensite, producing a finely divided mixture of α and β phase, resulting in increased strength [26,27]. In this study, solution treatment was performed under vacuum at 940 °C for 1 h followed by argon fast cooling and aged at 480 °C for 8 h followed by furnace cooling to room temperature.

(ii) Hot isostatic pressing (HIP): HIP is a widely accepted thermo-mechanical method for closing internal defects (except surface connected pores) in titanium castings or additively manufactured parts. In the HIP process, chemically cleaned parts were loaded inside a HIP chamber which later on was filled with high-purity argon gas to create high pressure (usually in the range of 70–205 MPa) and temperature (900–955 °C for titanium) for some fixed dwell time, e.g., 2–4 h. As the yield strength of the material drops at high temperatures, the application of pressure results in high diffusion rates and the plastic flow of the material, which helps to close any voids or microcracks [27,28]. In this study, HIP treatment was performed at 140 MPa and 930 °C for a duration of 4 h.

(iii) HIP followed by STA (HIP + STA): Several studies reported that HIP temperatures can coarsen α platelets, causing a reduction in tensile strength of the material. Therefore, to recover the strength of the material, STA treatment is generally performed after HIP [27,28]. Parameters used for HIP + STA treatment was the same as mentioned earlier for STA and HIP.

2.4. Microstructural Characterisation

For microstructural characterisation, specimens were cross-sectioned, followed by standard metallographic procedures, including mounting, grinding with SiC abrasive paper discs up to the grit size of 2500, and polishing using diamond suspension followed by final polishing with OP-U colloidal silica suspension (0.04 µm). Specimens were etched using Kroll's reagent (88% distilled water, 10% nitric acid, and 2% hydrofluoric acid) by immersion method for 10–15 s. Optical microscopy (Olympus BX41M-LED, Tokyo, Japan) and scanning electron microscopy or SEM (ZEISS EVO LS 15, Jena, Germany) were used to examine the microstructure of the etched and polished samples. For porosity measurement, a minimum of 20 optical micrographs were taken at 100–200× magnification from unetched specimens. They were analysed as per ASTM E2109 [29] using open-source ImageJ software 1.53t to automatically locate pores and calculate area fraction of porosity (%).

2.5. Evaluation of Mechanical Properties

Microhardness measurements were performed on polished cross-sections of CS deposits (in four conditions: AD, STA, HIP, HIP + STA) using a Zwick Microhardness Tester (ZwickRoell, Leominster, UK) with Vickers loads of 0.1 kg following ASTM E384 [30]. To calculate average values, a minimum of 20 measurements were performed throughout the thickness of the CS deposits. Nanoindentation measurements were also performed to compare the hardness of feedstock powder with both CS deposits and substrate. Nanoindentation was carried out using a Nanoindenter P3 (Micro Materials, Wrexham, UK) fitted with a diamond Berkovich indenter tip at a load of 10 mN. A minimum of 10 readings were taken for each specimen and then averaged. The relation ($H_V = 94.5 \times H_{IT}$) was used to convert hardness values from Indentation hardness (H_{IT}) in GPa to Vickers hardness (H_V) [31].

Tensile tests were conducted as per ASTM E8/E8M [32] for three different specimen types: (i) mill annealed Ti6Al4V, (ii) 'fully CS' Ti6Al4V material, and (iii) 'CS repair' specimens with two repair ratios 1:5 and 2:5. Here, repair ratio represents the ratio of CS deposits thickness to total specimen thickness (e.g., repair ratio 2:5 represents CS deposits thickness is 2 mm when the total specimen thickness is 5 mm). Specimens with the 1:5 repair ratio were tested only in AD condition, and specimens with the 2:5 repair ratio was tested both in AD and thermally treated conditions. Here, "fully CS" represents specimens extracted entirely from CS Ti6Al4V deposits, and "CS repair" means specimens that were extracted from a CS deposit-substrate assembly (CS Ti6Al4V deposited on Ti6Al4V substrate). The manufacturing steps of the repair tensile specimens are shown in Figure 1a. Fully CS specimens were extracted from an 8.5 mm thick CS Ti6Al4V plate (deposited on an Al 5083-0 alloy substrate) as shown in Figure 1b,c. Dimensions of tensile specimens are shown in Figure 1d,e. Overall dimensions of fully CS and mill annealed Ti6Al4V specimens for tensile testing are the same as in Figure 1d. Tensile tests (three samples for each condition) were conducted using a 100 kN Instron 8502 (Instron, High Wycombe, UK) in displacement control mode with an Axial Clip-on Extensometer (class 0.5), and properties were evaluated in terms of the yield strength (YS), ultimate tensile strength (UTS), and elongation (El). The elastic modulus (E) values were calculated as per the "numerical data method" following ASTM E111 [33] using the stress–strain data (up to 0.25% strain) obtained from tensile tests, although the test set-up was not dedicated for E measurements. E values were also measured by impulse excitation technique or IET (IMCE, Genk, Belgium) as per ASTM E1876 [34] to compare with the values predicted from tensile tests (for IET test set-up, see [25]). Fracture surfaces of tensile tested specimens were investigated using SEM to understand the failure and bonding mechanisms.

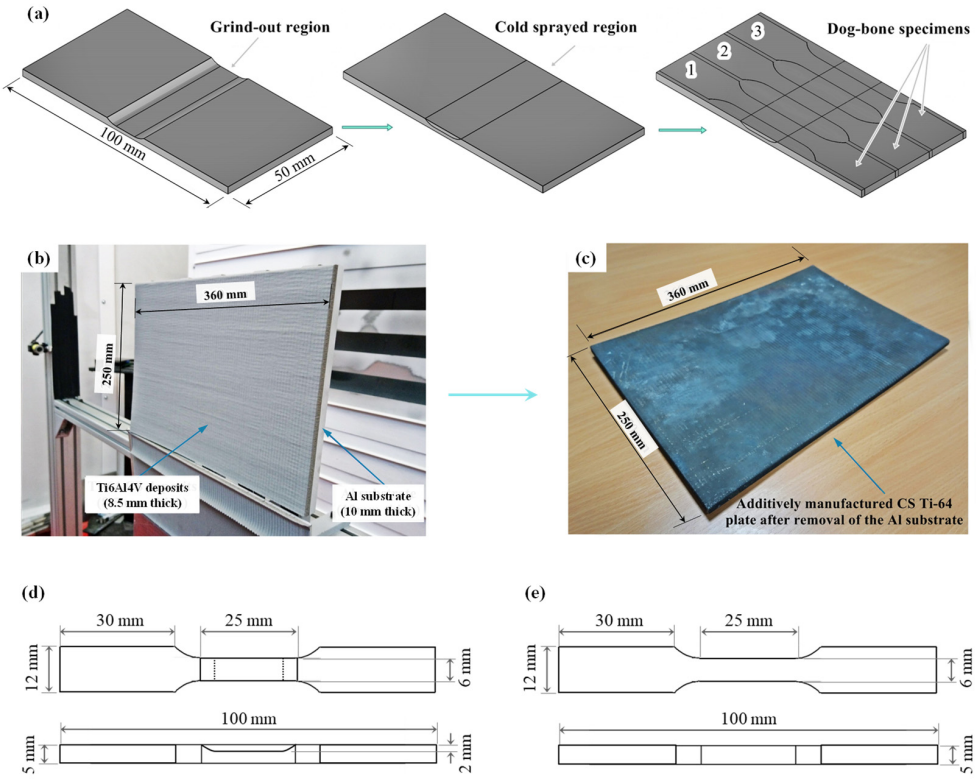

Figure 1. (**a**) Manufacturing steps of the repair tensile specimens; (**b**,**c**) manufacturing of the fully CS Ti6Al4V plate for extracting specimens for mechanical testing from 8.5 mm thick CS Ti6Al4V deposited on Al 5083-0 substrate, (**c**) a fully CS Ti6Al4V plate after removing the substrate; (**d**,**e**) dimensions of tensile specimens: (**d**) repair ratio 2:5, (**e**) fully CS.

3. Results

3.1. Microstructure and Porosity

SEM images of the cross-sections of CS deposited Ti6Al4V material in different conditions are present in Figure 2. In the AD condition (Figure 2a), the microstructure of CS deposits comprises severely deformed 'smooth' regions and partially deformed 'textured' regions inherited from the feedstock powder; whereas, the mesostructure comprises flattened powder particles that have undergone severe plastic deformation, along with process-induced porosity of 2.25 ± 0.16% (area fraction). Similar observations were also reported by other researchers [19,35–37]. The thermal treatments (for all cases: STA, HIP, and HIP + STA) led to complete disappearance of the microstructural features found in the AD condition through nucleation and growth of recrystallised grains in the regions of high energy, where dislocations are clustered at the particle interfaces due to severe impact of the powder particles during CS. This resulted in coarsened microstructure with equiaxed α grains (dark colour) with intergranular vanadium-rich β precipitates (light colour) as shown in Figure 2b–d. Both STA and HIP led to a decrease in porosity by around 21–23% from the AD condition (1.74 ± 0.10% after STA, 1.78 ± 0.16% after HIP) due to solid-state densification through atomic thermal diffusion and grain boundary migration at the inter-particle contact interfaces resulting in significant growth in metallurgical bonding between the deposited particles, which is favourable for mechanical properties. Nevertheless, the considerable porosity of 1.78% observed even after HIP might be due to surface-connected porosity or high open porosity leading to gas transfer between pores and hence insufficient material densification [15]. Conversely, HIP + STA treatments significantly increased porosity to 4.40 ± 0.35% from 1.78% in the HIP condition. Porosity regrowth during post-HIP heat treatment was also reported for selective electron beam melted Ti6Al4V in [38], which was reported to be due to pore expansion caused by the high pressure within the pores

which remained after HIP due to the low diffusivity of argon in titanium. The effect of various thermal treatments on the evolution of pore structure and microstructure has also been discussed elsewhere [3,14,17,19].

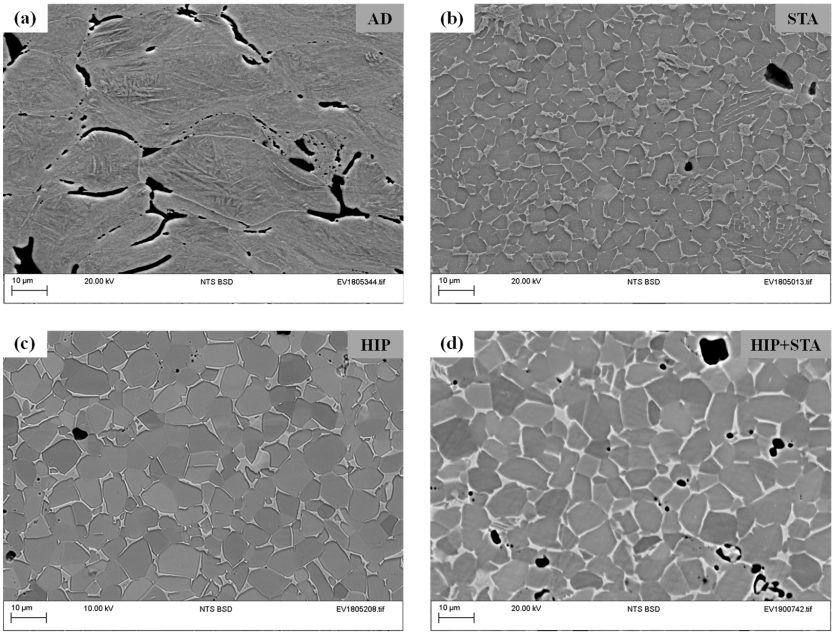

Figure 2. Cross-sectional SEM images of CS Ti6Al4V material for four conditions: (**a**) AD, (**b**) STA, (**c**) HIP, (**d**) HIP + STA.

3.2. Mechanical Properties

3.2.1. Hardness

The variation in hardness values of CS Ti6Al4V alloy in AD and after three different thermal treatments, plus a comparison with the feedstock powder and mill annealed substrate is shown in Figure 3. Hardness in the AD condition was found to be around 34% higher than that of the Ti6Al4V feedstock powder, and around 19–24% higher than the mill-annealed Ti6Al4V substrate. Higher hardness in the CS Ti6Al4V deposits (AD) was due to the work hardening effect associated with the severe plastic deformation of the sprayed particles, which is proportional to the impact velocity of the particles. Notably, the presence of porosity in CS deposits may lead to underestimation of the measured hardness values and can cause scattering of the data [14].

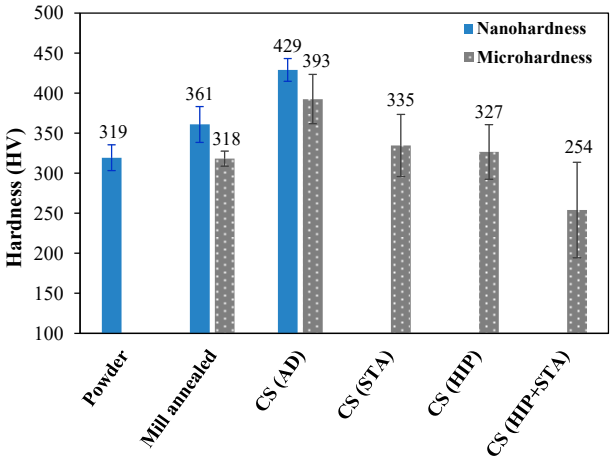

Figure 3. Comparison of average hardness values among CS Ti6Al4V deposits in various conditions (as-deposited and after thermal treatments), feedstock powder, and mill annealed Ti6Al4V substrate.

A decrease in hardness was observed as a result of various thermal treatments. After STA, HIP, and HIP + STA, hardness decreased by 15%, 17%, and 35%, respectively. Lower hardness after thermal treatments was due to the microstructural changes as a result of static recovery mechanisms during high-temperature annealing processes, transforming work hardened microstructure to equiaxed microstructure through recovery, recrystallization, and phase transformation [3,14]. High-temperature thermal treatments promoted the growth of β phase vanishing the 'smooth' and 'textured' regions of CS Ti6Al4V deposits possessed in the AD condition [14]. For HIP + STA treated specimens, a significant decrease in hardness (35% reduction from that of the AD condition) was observed, which was attributed to the observed increase in porosity.

3.2.2. Tensile Properties

Tensile properties for fully CS and CS repair specimens are presented in Figure 4 for four different conditions, i.e., AD, STA, HIP, and HIP + STA. Figure 4a,b show the stress–strain relationship for fully CS and CS repair specimens, respectively. Figure 4c–e showing values of *E*, UTS, and elongation. In the AD condition, fully CS specimens failed in a brittle manner at 287 ± 7 MPa UTS and 0.44% elongation with no yield point. The *E* value calculated from the stress–strain curve for the fully CS Ti-64 (AD) was found to be 76 GPa, which was about 32% lower than the mill annealed Ti6Al4V (112 GPa). However, from the IET measurements, *E* obtained for CS Ti6Al4V AD material (88 GPa) was around 16% higher than the values obtained from the stress–strain curve (76 GPa).

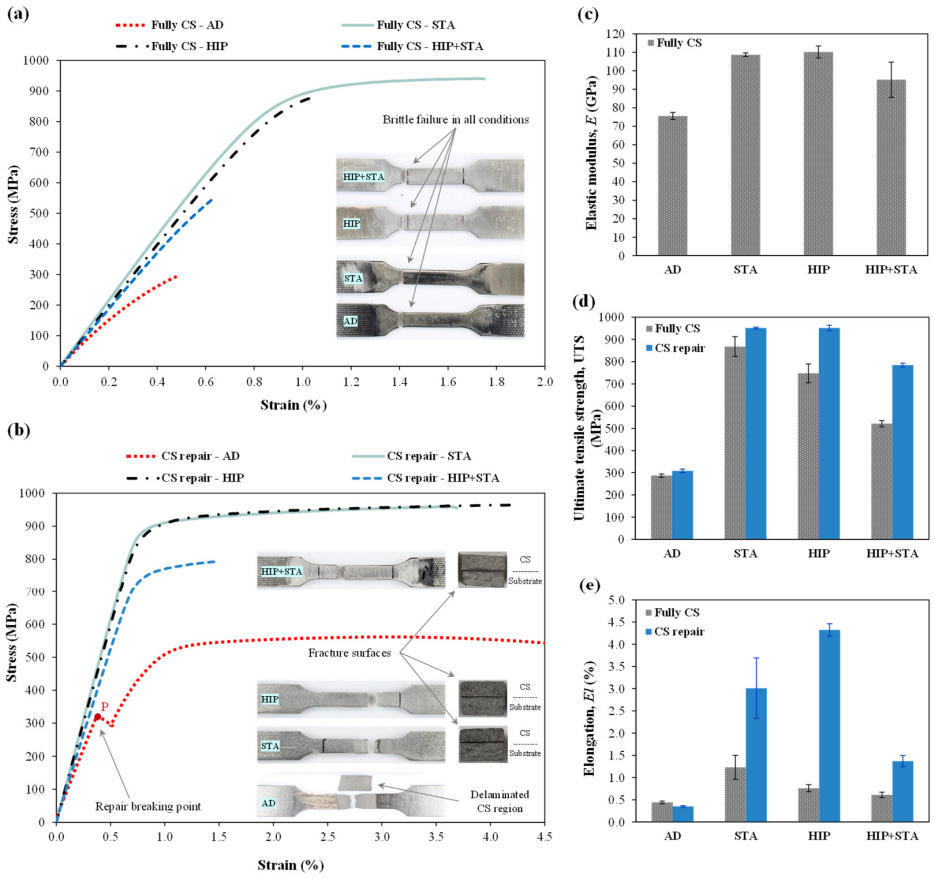

Figure 4. Tensile properties in four different conditions, i.e., AD, STA, HIP, and HIP + STA: (**a**) fully CS specimen: stress–strain curves, (**b**) CS repair specimen with 2:5 repair ratio: stress–strain curves, comparison among (**c**) elastic moduli of fully CS material calculated from the stress–strain curve, (**d**) ultimate tensile strength, and (**e**) elongation.

Thermal treatments significantly improved tensile properties. For the fully CS material, STA led to the most improved tensile properties among the investigated cases. In the STA condition, UTS increased by about 202% (from 287 to 868 MPa); *E* increased by 43% (from 76 to 109 GPa), which is close to the value of mill annealed Ti6Al4V. Elongation increased by 180% (from 0.44% to 1.23%), however, the elongation values were significantly lower than that of the wrought counterpart in mill annealed condition (14%). Only mild elastic-plastic deformation was found for the specimens with STA, yielding at around 880 MPa, i.e., 0.2% offset YS (only observed in one out of three specimens). Notably, STA also resulted in significant improvement in interfacial adhesion strength by more than 520% reaching 766 MPa (from 122 MPa in the AD condition), as reported in our previous work [23]. More information on interfacial adhesion strength of CS Ti6Al4V deposited to Ti6Al4V substrates can be found in [24].

For CS repair specimens, a sudden shift in the stress–strain curve (Figure 4b) was observed, as marked by point 'P'. This was the region where the repair had broken into two pieces as shown in the offset, then gradually started delaminating from the substrate leading to complete delamination (i.e., the CS part of the repair-substrate assembly). Until the breaking point 'P', the slope on the stress–strain curve is a contribution of both the parent material and the CS deposited material. However, after breaking point 'P', the drop in tensile stress was partially recovered by the substrate material and the remaining stress–strain plot including the plastic region arose from the strain hardening of the substrate only. The actual stress–strain representation of the repair/substrate system is just up to the point where the CS coating fails, therefore, the UTS of the CS repair specimen is represented by point 'P'. A comparison of tensile properties between specimens with two repair ratios (1:5 and 2:5) is presented in Appendix A.

Similar to fully CS material, tensile properties of the CS repair specimens were significantly improved after thermal treatments. It was found that UTS increased by more than 200% from 308 MPa in the AD condition to 951 MPa after both STA, and HIP. Moreover, the HIP improved elongation from 0.35% to 4.32%. Higher values in the case of CS repair specimens as compared to fully CS material is due to the contribution of the parent material towards the overall properties, mainly for elongation values. However, it is not clear how much contribution the parent material has towards the final results, which requires further investigation.

Figure 5 compares the fracture surfaces of tensile tested specimens in four different conditions. As shown in Figure 5a, failure happened in a brittle fracture manner in the AD condition which was mainly due to debonding at the mechanically interlocked particle boundaries, leaving a smooth crater or cleavage fracture along the inter-particle interfaces (although there were few localised ductile dimples observed on the fracture surface). The presence of uniformly distributed process-induced porosity resulting from undeformed particles and lack of mechanical interlocking in between deposited particles [7,14] was also deemed to have contributed to the failure mechanism. After thermal treatments (Figure 5b–d), the proportion of ductile features on the fracture surface significantly increased due to the formation of metallurgical bonding, thereby enhancing tensile strength when compared with the AD condition. However, thermal treatments had less influence on the ductility of the material, as process-induced porosity was not sufficiently reduced and hence no significant improvement in elongation was obtained. CS region of the repair specimens also showed similar characteristics as the fully CS specimens, and did not bring any different observations. Therefore, it is not presented here.

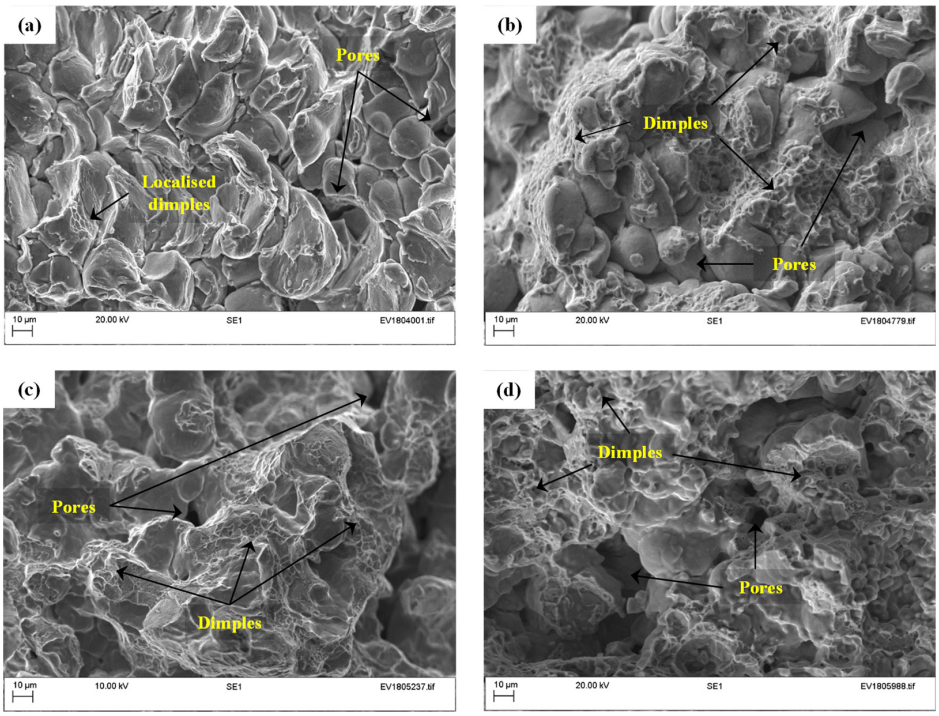

Figure 5. SEM images of fracture surfaces of fully CS tensile specimens in four different conditions: (**a**) AD, (**b**) STA, (**c**) HIP, and (**d**) HIP + STA.

4. Discussion

4.1. Overview

Tensile properties of CS Ti6Al4V were found to be poor in the AD condition, caused by the presence of highly deformed cold worked particles with weak inter-particle bonding and considerable process-induced porosity (2.25%), even after using high process gas temperature and pressure (1100 °C and 5 MPa). Post-deposition thermal treatments resulted in significant improvement in tensile properties, which was mainly attributed to improve metallurgical bonding due to atomic diffusion and grain boundary migration (supported by fractography and microstructural analysis). However, none of the thermal treatments performed in this study was successful in fully closing the process-induced porosity, hence the very low elongation (highest being 1.23% after STA).

Data collected from the open literature [3,8–11,13–16] on the effect of various thermal treatments on tensile properties also suggest more or less similar findings as this study, as summarised in Table 2 and Figure 6.

Table 2. Tensile properties of fully cold spray deposited Ti6Al4V reported in the literature, and data generated from this study.

Process Gas	Temperature (°C)/Pressure (MPa)	Testing Condition	Porosity (%)	UTS (MPa)	Elongation (%)	*E* (GPa)	Measurement Method	References (et al.)
He	450–530/2.4	As-deposited Annealing [a1] Encapsulated HIP [b1]	18–26 18–26 ~0	52–109 236–244 890–1024	0.16–0.48 0.64–0.68 12.3–14.0	28 61 115	ASTM E8 (sub-size round)	Blose [13]
	350/4	As-deposited Annealing [a2]	~0.3 ~0.3	445 ± 145 764 ± 189	3.8 ± 0.8 * 6.3 ± 0.5 *	- -	MFT [e1]	Vo [3]
	950/2	As-deposited HIP [b2]	~1.2 ~0.04	373 ± 10 962 ± 31	~0.46 ~1.76	75 80	ASTM E8 (sub-size flat)	Chen [14]

Table 2. *Cont.*

Process Gas	Temperature (°C)/Pressure (MPa)	Testing Condition	Porosity (%)	UTS (MPa)	Elongation (%)	*E* (GPa)	Measurement Method	References (et al.)
N_2	800/4	As-deposited Annealing [a3]	~6.7 ~6.7	~160 ~160	- -	- -	MFT [e1]	Wong [8]
	800/4	As-deposited Annealing [a4] Annealing [a5] Annealing [a6]	5–12 5–12 5–12 5–12	154 ± 81 251–273 144–219 180–462	2.3 ± 0.9 * 3.2–4.7 * 2.2–3.5 * 3.0–5.8 *	- - - -	MFT [e1]	Vo [3]
	800–1000/4–5	As-deposited	4.6–10.4	182–263 157–295	- -	- -	TCT [e2] MFT [e1]	List [9]
	950/5	As-deposited HIP [b2]	~2.4 ~1.5	85 ± 3 664 ± 21	~0.27 ~1.40	31 55	ASTM E8 (sub-size flat)	Chen [14]
	950/4.5	As-deposited	4–5	337 ± 17	4.4–5.3 *	-	MFT [e1]	Tan [10]
	600/5	As-deposited Encapsulated HIP [b3]	7.5 0.2	68 ± 5 956 ± 5	0.54 13.5 ± 0.5	99 99	ASTM E8 (sub-size flat)	Petrovskiy [15]
	800/4	As-deposited HIP [b4]	~6.5 4.9–5.2	105 635	0.65 0.97	- -	ASTM E8 (sub-size flat)	Petrovskiy [16]
-	-	As-deposited HIP [b5] HSPT [c1]	- - -	147 798 859	0.24 2.5 3.1	61 86 91	MFT specimen with DIC [e3]	Ligda [11]
N_2	1100/5	As-deposited STA [d1] HIP [b6] HIP [b6] + STA [d1]	2.25 1.74 1.78 4.40	287 ± 7 868 ± 44 747 ± 42 521 ± 14	0.44 ± 0.03 1.23 ± 0.27 0.76 ± 0.08 0.61 ± 0.08	77 ± 2 109 ± 1 110 ± 3 95 ± 10	ASTM E8 (sub-size flat)	This study

[a1] Annealing at 840 °C for 4 h and then air-cooled to room temperature; [a2] Annealing at 600 °C for 2 h; [a3] Annealing at 200, 400 °C for 4 h; [a4] Annealing at 600 °C for 0.5 and 1 h; [a5] Annealing at 200, 400, and 600 °C for 2 h; [a6] Annealing at 200, 400, 840, and 1000 °C for 4 h; [b1] Encapsulated hot isostatic pressing in a can at 900 ± 15 °C and 103 MPa for 2 h; [b2] Hot isostatic pressing at 920 °C and 120 MPa for 2 h; [b3] Encapsulated hot isostatic pressing at 900 °C and 110 MPa for 2 h; [b4] Hot isostatic pressing at 910 °C and 150 MPa for 2 h; [b5] Hot isostatic pressing: parameters unknown; [b6] Hot isostatic pressing at 930 °C and 140 MPa for 4 h; [c1] Hydrogen sintering and phase transformation at 1050–1200 °C for 1–8 h depending on the starting porosity; [d1] Solution treatment at 940 °C for 1 h and aged at 480 °C for 8 h; [e1] Micro flat tensile (MFT) [39]; [e2] Tubular coating tensile [12]; [e3] Digital image correlation (DIC) for strain calculations with a 12-megapixel camera (gauge Section 0.7 × 0.5 × 5 mm) [11]; * Actual values might be lower by 70–115% due to the use of MFT test; Note: WebPlotDigitizer 4.5, Oakland, CA, USA [40] was used to extract some of the data presented in this table.

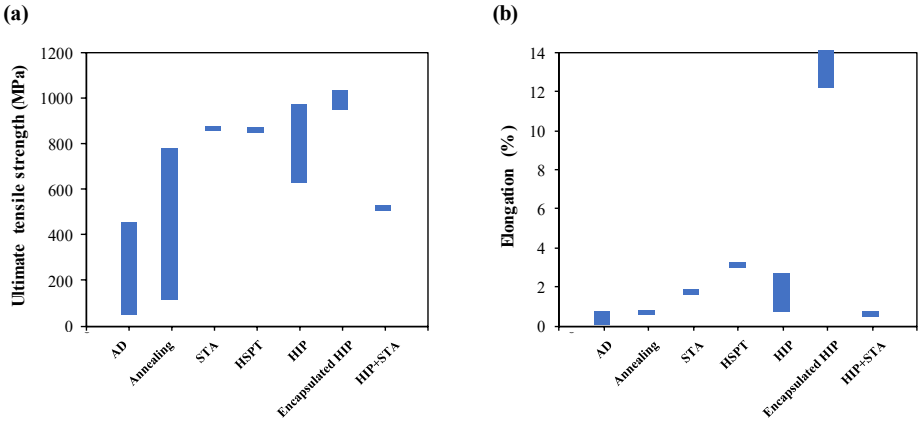

Figure 6. Effect of various post-deposition thermal treatments on improving tensile properties of fully CS deposited Ti6Al4V alloy (data collated from literature [3,8–11,13–16] and this study): (**a**) ultimate tensile strength (UTS), (**b**) elongation. (**a**,**b**) presents the range of UTS and elongation values for various testing conditions: as-deposited (AD), annealing, solution treatment and ageing (STA), hydrogen sintering and phase transformation (HSPT), hot isostatic pressing (HIP), encapsulated HIP, and HIP + STA.

4.2. Effect of Thermal Treatments on Ultimate Tensile Strength

From Table 2, it can be observed that the tensile strength of the fully CS Ti6Al4V material is very poor in the AD condition, although there was a slight improvement in the properties with the increase in process gas temperature and pressures. In the AD condition, UTS values were in the range of 68–337 MPa when using N_2 as process gas with temperature and pressure in the range of 600–1100 °C, and 4–5 MPa, respectively. On the other hand, when using He as process gas at 350–950 °C and 2–4 MPa, UTS values were recorded in the range of 52–445 MPa.

Tensile strengths were found to be significantly improved after thermal treatments, such as annealing [3,13], HIP [11,13–16], and hydrogen sintering and phase transformation (HSPT) [11]. Blose [13] reported that annealing at 840 °C for 4 h improved the UTS values from 52 to 236 MPa (manufactured using gas atomised powder), and from 109 to 244 MPa (manufactured using plasma atomised powder), sprayed using He in both cases. Vo et al. [3] performed several annealing treatments with temperature ranging from 200 to 1000 °C for 0.5 to 5 h. For He sprayed specimens, the best result reported was an improvement of UTS value from 445 to 764 MPa after annealing at 600 °C for 2 h. For N_2 sprayed specimens UTS increases from 180 to 462 MPa after annealing at 1000 °C for 4 h.

Regarding HIP treatment, Blose [13] reported that encapsulated HIP (900 °C and 103 MPa for 2 h) significantly improved UTS values up to 1024 MPa (deposited using He). Similarly, after a standard (capsule free) HIP treatment at 920 °C and 120 MPa for 2 h, Chen et al. [14] found improvement in UTS values from 373 to 962 MPa (He as process gas) and 85 to 664 MPa (N_2 as process gas). Likewise, Ligda et al. [11] reported an increase in UTS from 147 to 798 MPa after standard HIP treatment. In the same study, an increase in UTS from 147 to 859 MPa was reported after HSPT treatment. Most recently, Petrovskiy et al. [16] stated an increase in UTS from 105 to 635 MPa (deposited using N_2) after standard HIP treatment. Another study by Petrovskiy et al. [15] reported improvement in UTS from 68 to 956 MPa (deposited using N_2) after encapsulated HIP treatment at 900 °C and 110 MPa for 2 h.

4.3. Effect of Thermal Treatments on Elongation

Although significant improvements in tensile strength were observed after thermal treatments, elongation of the CS Ti6Al4V material remained very low in most of the cases. Tests performed using ASTM E8 (sub-size specimens) showed no more than 0.48% elongation in the AD condition irrespective of the spraying conditions as reported by Blose [13] and Chen et al. [14]. Similarly, strain calculations performed using DIC (digital image correlation) by Ligda et al. [11] also showed elongation around 0.24%. In contrast, tests performed using Micro Flat Tensile (MFT) test showed comparatively higher elongation even in the AD condition, which were reported to be 2.3–3.8% (by Vo et al. [3]) and 4.4–5.3% (Tan et al. [10]). Elongation for CS deposited material having ~2.4% porosity was reported to be ~0.27% [14] when tested using ASTM E8; on the other hand, when tested using MFT, CS deposits with higher porosities of 8.1% and 4–5% reported having higher elongation of ~2.3% [3], and 4.4–5.3% [10], respectively. Moreover, using MFT test, elongation of wrought Ti6Al4V was also found to be around 25.7% by Vo et al. [3], which is around 2 times higher than the standard value of wrought Ti6Al4V (mill annealed). At room temperature, typical elongation value of Ti6Al4V alloy would be expected to be around 12–15% (~12% in sheet form, ~15% in bar form) [41]. Therefore, it can be assumed that the actual elongation values for CS Ti6Al4V material is significantly lower (approximately, half of the measured values) when obtained from the MFT test. This might be due to error in strain measurements as test specimens with smaller dimensions increase the sensitivity of the results.

It is important to note that irrespective of testing methods, no significant improvement in elongation was observed after thermal treatments (such as annealing [3,8,13], standard HIP [11,14,16] or HSPT [11]); except the "encapsulated HIP" treatment by Blose [13] and Petrovskiy et al. [15]. Encapsulated HIP reduced porosity from 18–24% to almost 0%

reported by Blose [13], and from 7.5% to 0.2% reported by Petrovskiy et al. [15]. As a result, elongation was improved to 13.5–14% after HIP.

4.4. Effect of Thermal Treatments on Elastic Modulus

Elastic modulus (*E*) values presented in Table 2 were determined from the elastic response region of the stress versus strain plots (up to 0.25% strain) reported in the literature by extracting stress and strain values using the WebPlotDigitizer, 4.5, Oakland, CA [40]. It was found that suitable thermal treatments can improve *E* up to 115 GPa (after HIP by Blose [13] when porosity was reduced close to zero), which is close to the value of wrought Ti6Al4V. *E* values determined from the stresss-train relations reported by Chen et al. [14] and Ligda et al. [11] also showed improvement after HIP and HSPT treatments.

4.5. Key Takeaways

The lower tensile strength, elastic modulus, and elongation in CS deposited Ti6Al4V is mainly due to the presence of porosity and highly deformed cold worked particles with weak inter-particle bonding between deposited particles [3,8,13]. Improvement in tensile strength after various thermal treatments were mainly due to an increase in cohesion strength between deposited particles due to the formation of metallurgical inter-particle diffusion bonding, homogenisation of microstructure and in some cases reduction in porosity (especially for HIP treated specimens). However, porosity remained relatively unchanged after annealing treatments [3,13].

The "standard HIP" treatment used in this study and also by Ligda et al. [11], Chen et al. [14], and Petrovskiy et al. [16] were not successful due to the presence of surface connected pores. To resolve the porosity issue, the "encapsulated HIP" can be used. Encapsulated HIP can reduce porosity close to zero percentage irrespective of the original porosity content in the AD condition. To support this, there are two examples of CS Ti6Al4V, Bolse [13] reduced porosity form 18–24% to ~0%, and more recently Petrovskiy et al. [15] reduced from 7.5% to 0.2%. As a result, elongation improved to 14%.

5. Conclusions

This study investigated the effect of three different post-deposition thermal treatments (solution treatment and ageing (STA), hot isostatic pressing (HIP), and HIP followed by STA (HIP + STA)) on the tensile properties of fully cold spray (CS) Ti6Al4V and CS Ti6Al4V repairs. In addition, the CS deposited material was characterised in terms of microstructure, porosity, and hardness. The following conclusions can be drawn based on this study:

1. Post-deposition thermal treatments led to complete disappearance of the microstructural features found in the as-deposited condition, resulting in coarsened microstructure having equiaxed α grains with intergranular β precipitates. Porosity (in terms of area fraction) was reduced from 2.3% in the as-deposited condition to 1.7% after STA, and/or HIP treatment.
2. STA and HIP treatments lowered hardness by 15–17% due to microstructural softening in the CS deposits caused by static recovery mechanisms during high-temperature thermal treatments.
3. Post-deposition thermal treatments resulted in significant improvement in the tensile strength, which is mainly attributed to increase in cohesion strength between deposited particles due to improved metallurgical inter-particle diffusion bonding, homogenisation of microstructure, and in some cases reduction in porosity. For the fully CS material, the ultimate tensile strength (UTS) was improved the most by around 200%, from 287 MPa in AD to 868 MPa after STA.
4. Elongation was much lower for all investigated cases with the highest measured value (averaged) of 1.23% after STA.
5. For CS repair specimens (repair ratio 2:5), both STA and HIP treatments improved the UTS by 209%, from 308 to 951 MPa, elongation from 0.35% to 3.01% after STA, and to 4.32% after HIP. Better performance in repair specimens (compared to fully CS

specimens) could be due to the contribution of the substrate material (mil annealed Ti6Al4V) towards the overall performance.

Author Contributions: Conceptualization, D.B. and X.Z.; methodology, D.B., X.Z., P.M. and R.K.; formal analysis, D.B.; investigation, D.B.; data curation, D.B.; writing—original draft preparation, D.B.; writing—review and editing, D.B., X.Z., H.B., R.K.; visualization, D.B.; supervision, X.Z.; funding acquisition, X.Z. All authors have read and agreed to the published version of the manuscript.

Funding: This work was supported by Lloyd's Register Foundation under the Grant number DB012017COV; and Coventry University under the grant number 7486157.

Institutional Review Board Statement: Not applicable.

Informed Consent Statement: Not applicable.

Data Availability Statement: Not applicable.

Acknowledgments: This research was enabled through and undertaken at the National Structural Integrity Research Centre, a postgraduate engineering facility for industry-led research into structural integrity established and managed by TWI Ltd. This work was sponsored by the Lloyd's Register Foundation, a charitable organization that helps to protect life and property by supporting engineering-related education, public engagement and the application of research. Authors would like to thank Matthew Dore from TWI Ltd. and Abdul Khadar Syed from Coventry University for their support in various phases of this project.

Conflicts of Interest: The authors declare no conflict of interest. The funders had no role in the design of the study; in the collection, analyses, or interpretation of data; in the writing of the manuscript; or in the decision to publish the results.

Appendix A. Tensile Strength for Specimens with Different Repair Ratios

Figure A1 compares the tensile properties of mill annealed Ti6Al4V, fully CS Ti6Al4V, and CS repaired specimens with two repair ratios (2:5 and 1:5). It was observed that the UTS of the 2:5 repair is very close to fully CS material, but in the case of 1:5, UTS value is higher. Which is due to the higher resistance provided by the thicker substrate material against the tensile loading.

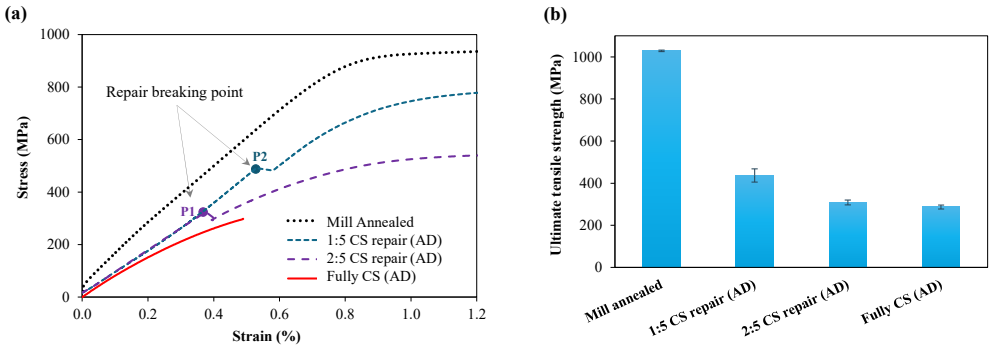

Figure A1. A comparison of tensile properties among mill annealed Ti6Al4V, fully CS Ti6Al4V, and CS repairs (repair ratios 2:5 and 1:5) in AD condition: (**a**) strain-strain curves, (**b**) UTS values.

References

1. Boyer, R.R. An overview on the use of titanium in the aerospace industry. *Mater. Sci. Eng. A* **1996**, *213*, 103–114. [CrossRef]
2. Inagaki, I.; Takechi, T.; Shirai, Y.; Ariyasu, N. *Application and Features of Titanium for the Aerospace Industry*; Nippon Steel: Shimaya, Japan, 2014.
3. Vo, P.; Irissou, E.; Legoux, J.-G.; Yue, S. Mechanical and Microstructural Characterization of Cold-Sprayed Ti-6Al-4V After Heat Treatment. *J. Therm. Spray Technol.* **2013**, *22*, 954–964. [CrossRef]
4. Li, W.; Cao, C.; Yin, S. Solid-state cold spraying of Ti and its alloys: A literature review. *Prog. Mater. Sci.* **2019**, *110*, 100633. [CrossRef]

5. Sova, A.; Grigoriev, S.; Okunkova, A.; Smurov, I. Potential of cold gas dynamic spray as additive manufacturing technology. *Int. J. Adv. Manuf. Technol.* **2013**, *69*, 2269–2278. [CrossRef]
6. Blose, R.; Walker, B.; Walker, R.; Froes, S. New opportunities to use cold spray process for applying additive features to titanium alloys. *Met. Powder Rep.* **2006**, *61*, 30–37. [CrossRef]
7. Boruah, D. Structural Integrity Assessment of Cold Spray Additive Manufactured Titanium Alloy Ti-6Al-4V. Ph.D. Thesis, Coventry University, Coventry, UK, 2020.
8. Wong, W.; Irissou, E.; Legoux, J.G.; Vo, P.; Yue, S. Powder Processing and Coating Heat Treatment on Cold Sprayed Ti-6Al-4V Alloy. *Mater. Sci. Forum* **2012**, *706–709*, 258–263. [CrossRef]
9. List, A.; Lyphout, C.; Villa, M.; Gärtner, F.; Klassen, T. Mechanical Properties of Cold-Sprayed Ti-6Al-4V Coatings. In Proceedings of the International Thermal Spray Conference and Exposition: Innovative Coating Solutions for the Global Economy, ITSC 2013, Busan, Korea, 13–15 May 2013.
10. Tan, A.W.-Y.; Sun, W.; Bhowmik, A.; Lek, J.Y.; Song, X.; Zhai, W.; Zheng, H.; Li, F.; Marinescu, I.; Dong, Z.; et al. Effect of Substrate Surface Roughness on Microstructure and Mechanical Properties of Cold-Sprayed Ti6Al4V Coatings on Ti6Al4V Substrates. *J. Therm. Spray Technol.* **2019**, *28*, 1959–1973. [CrossRef]
11. Ligda, J.P.; Butler, B.G.; Saenz, N.; Paramore, J. Mechanical Behavior of Additively Manufactured Ti-6Al-4V Following a New Heat Treatment. In *Mechanics of Additive and Advanced Manufacturing*; Kramer, S., Jordan, J.L., Jin, H., Carroll, J., Eds.; Springer International Publishing: Cham, Switzerland, 2019; pp. 29–30.
12. Schmidt, T.; Gärtner, F.; Kreye, H. *Tubular-Coating-Tensile-Test*; Helmut Schmidt University: Hamburg, Germany, 2006.
13. Blose, R.E. Spray Forming Titanium Alloys Using the Cold Spray Process. In Proceedings of the International Thermal Spray Conference, ASM International, Basel, Switzerland, 2–4 May 2005.
14. Chen, C.; Xie, Y.; Yan, X.; Yin, S.; Fukanuma, H.; Huang, R.; Zhao, R.; Wang, J.; Ren, Z.; Liu, M.; et al. Effect of hot isostatic pressing (HIP) on microstructure and mechanical properties of Ti6Al4V alloy fabricated by cold spray additive manufacturing. *Addit. Manuf.* **2019**, *27*, 595–605. [CrossRef]
15. Petrovskiy, P.; Travyanov, A.; Cheverikin, V.V.; Chereshneva, A.A.; Sova, A.; Smurov, I. Effect of encapsulated hot isostatic pressing on properties of Ti6Al4V deposits produced by cold spray. *Int. J. Adv. Manuf. Technol.* **2020**, *107*, 437–449. [CrossRef]
16. Petrovskiy, P.; Khomutov, M.; Cheverikin, V.; Travyanov, A.; Sova, A.; Smurov, I. Influence of hot isostatic pressing on the properties of 316L stainless steel, Al-Mg-Sc-Zr alloy, titanium and Ti6Al4V cold spray deposits. *Surf. Coat. Technol.* **2021**, *405*, 126736. [CrossRef]
17. Zhou, H.; Li, C.; Yang, H.; Luo, X.; Yang, G.; Li, W.; Hussain, T.; Li, C. Pores Structure Change Induced by Heat Treatment in Cold-Sprayed Ti6Al4V Coating. *J. Therm. Spray Technol.* **2019**, *28*, 1199–1211. [CrossRef]
18. Khun, N.W.; Tan, A.W.Y.; Sun, W.; Liu, E. Effect of Heat Treatment Temperature on Microstructure and Mechanical and Tribological Properties of Cold Sprayed Ti-6Al-4V Coatings. *Tribol. Trans.* **2016**, *60*, 1033–1042. [CrossRef]
19. Bhowmik, A.; Tan, A.W.; Sun, W.; Wei, Z.; Marinescu, I. On the heat-treatment induced evolution of residual stress and remarkable enhancement of adhesion strength of cold sprayed Ti-6Al-4V coatings. *Results Mater.* **2020**, *7*, 100119. [CrossRef]
20. Li, W.Y.; Zhang, C.; Guo, X.; Xu, J.; Li, C.J.; Liao, H.; Coddet, C.; Khor, K.A. Ti and Ti-6Al-4V coatings by cold spraying and microstructure modification by heat treatment. *Adv. Eng. Mater.* **2007**, *9*, 418–423.
21. Bhattiprolu, V.S.; Johnson, K.W.; Crawford, G.A. Influence of Powder Microstructure on the Microstructural Evolution of As-Sprayed and Heat Treated Cold-Sprayed Ti-6Al- 4V Coatings. *J. Therm. Spray Technol.* **2019**, *28*, 174–188. [CrossRef]
22. Garrido, M.; Sirvent, P.; Poza, P. Evaluation of mechanical properties of Ti6Al4V cold sprayed coatings. *Surf. Eng.* **2017**, *34*, 399–406. [CrossRef]
23. Boruah, D.; Zhang, X. Effect of Post-Deposition Solution Treatment and Ageing on Improving Interfacial Adhesion Strength of Cold Sprayed Ti6Al4V Coatings. *Metals* **2021**, *11*, 2038. [CrossRef]
24. Boruah, D.; Robinson, B.; London, T.; Wu, H.; de Villiers-Lovelock, H.; McNutt, P.; Doré, M.; Zhang, X. Experimental evaluation of interfacial adhesion strength of cold sprayed Ti-6Al-4V thick coatings using an adhesive-free test method. *Surf. Coat. Technol.* **2019**, *381*, 125130. [CrossRef]
25. Boruah, D.; Ahmad, B.; Lee, T.L.; Kabra, S.; Syed, A.K.; McNutt, P.; Doré, M.; Zhang, X. Evaluation of residual stresses induced by cold spraying of Ti-6Al-4V on Ti-6Al-4V substrates. *Surf. Coat. Technol.* **2019**, *374*, 591–602. [CrossRef]
26. Gupta, R.K.; Kumar, V.A.; Chhangani, S. Study on Variants of Solution Treatment and Aging Cycle of Titanium Alloy Ti6Al4V. *J. Mater. Eng. Perform.* **2016**, *25*, 1492–1501. [CrossRef]
27. Matthew, J.; Donachie, J. Heat treating titanium and its alloys. *Heat Treat. Prog.* **2001**, *1*, 47–57.
28. Soundarapandiyan, G.; Chen, B.; Fitzpatrick, M. Effect of postprocessing thermal treatments on electron-beam powder bed–fused Ti6Al4V. *Mater. Des. Process. Commun.* **2020**, *3*, 1–8. [CrossRef]
29. *ASTM E2109-01*; Standard Test Methods for Determining Area Percentage Porosity in Thermal Sprayed Coatings. ASTM Int.: West Conshohocken, PA, USA, 2014.
30. *ASTM E384-17*; Standard Test Method for Microindentation Hardness of Materials. ASTM Int.: West Conshohocken, PA, USA, 2017.
31. *ISO 14577-1*; Metallic Materials—Instrumented Indentation Test for Hardness and Materials Parameters—Part 1: Test Method. ISO: Geneva, Switzerland, 2015.
32. *ASTM E8/E8M-16a*; Standard Test Methods for Tension Testing of Metallic Materials. ASTM Int.: West Conshohocken, PA, USA, 2016.
33. *ASTM E111-17*; Standard Test Method for Young's Modulus, Tangent Modulus, and Chord Modulus. ASTM Int.: West Conshohocken, PA, USA, 2017.

34. *ASTM E1876-15*; Standard Test Method for Dynamic Young's Modulus, Shear Modulus, and Poisson's Ratio by Impulse Excitation of Vibration. ASTM Int.: West Conshohocken, PA, USA,, 2015.
35. Lek, J.Y.; Bhowmik, A.; Tan, A.W.Y.; Sun, W.; Song, X.; Zhai, W.; Buenconsejo, P.J.; Li, F.; Liu, E.; Lam, Y.M.; et al. Understanding the microstructural evolution of cold sprayed Ti-6Al-4V coatings on Ti-6Al-4V substrates. *Appl. Surf. Sci.* **2018**, *459*, 492–504. [CrossRef]
36. Birt, A.M.; Champagne, V.K.; Sisson, R.D.; Apelian, D. Microstructural Analysis of Cold-Sprayed Ti-6Al-4V at the Micro- and Nano-Scale. *J. Therm. Spray Technol.* **2015**, *24*, 1277–1288. [CrossRef]
37. Tan, A.W.-Y.; Sun, W.; Bhowmik, A.; Lek, J.Y.; Marinescu, I.; Li, F.; Khun, N.W.; Dong, Z.; Liu, E. Effect of coating thickness on microstructure, mechanical properties and fracture behaviour of cold sprayed Ti6Al4V coatings on Ti6Al4V substrates. *Surf. Coat. Technol.* **2018**, *349*, 303–317. [CrossRef]
38. Tammas-Williams, S.; Withers, P.; Todd, I.; Prangnell, P. Porosity regrowth during heat treatment of hot isostatically pressed additively manufactured titanium components. *Scr. Mater.* **2016**, *122*, 72–76. [CrossRef]
39. Gärtner, F.; Stoltenhoff, T.; Voyer, J.; Kreye, H.; Riekehr, S.; Koçak, M. Mechanical properties of cold-sprayed and thermally sprayed copper coatings. *Surf. Coat. Technol.* **2006**, *200*, 6770–6782. [CrossRef]
40. WebPlotDigitizer v4.5. Extract Data from Plots, Images, and Maps, (n.d.). Oakland, CA, USA, 2022. Available online: https://automeris.io/WebPlotDigitizer/ (accessed on 2 January 2020).
41. Rice, R.C.; Jackson, J.L.; Bakuckas, J.; Thompson, S. *Metallic Materials Properties Development and Standardization (MMPDS)*; SAE: Springfield, VA, USA, 2003.